Minimal Energy Dissipation Rate and Director Orientation Relative to External Dissipative Fields such as Temperature and Velocity Gradients in Nematic and Cholestric Liquid Crystals

Sten Sarman [*], **Yonglei Wang, Aatto Laaksonen**

Department of Materials and Environmental Chemistry
Arrhenius Laboratory, Stockholm University
106 91 Stockholm, Sweden

*E-mail: sarman@ownit.nu

Abstract: The purpose of this review article is to summarize observations accumulated over the years on director alignment phenomena in nematic and cholesteric liquid crystals by molecular dynamics simulation of molecular model systems and by experiment on real systems. The main focus is on the alignment angle between the director and external dissipative fields such as velocity gradients in various flow geometries and temperature gradients doing irreversible work on the system. A general observation is that the director attains an orientation relative to the field where the energy dissipation rate is minimal in the steady state. In the case of planar elongational flow, it can be proven by using symmetry arguments that the energy dissipation rate must be either maximal or minimal and simulations have shown that is minimal. In planar Couette flow both simulations and experiments imply that the energy dissipation rate is minimal in the steady state. Finally, in the case of heat conduction, symmetry arguments imply that the energy dissipation rate must be either minimal or maximal and simulations and experiments indicate that it is minimal. All these observations can be explained by applying a recently proven theorem according to which the energy dissipation rate is minimal in the steady state in the linear regime at low fields.

Key words: Liquid crystals, nonequilibrium molecular dynamics simulation, shear flow, elongational flow, heat conduction, alignment phenomena, minimal energy dissipation rate

I. INTRODUCTION

Liquid crystals consist of rod-like or disk-like molecules with varying orientational and translational order and they can be regarded as a state between the solid and liquid states. The simplest kind of liquid crystal is the nematic liquid crystal [1, 2], where there is an average orientation of the molecules in a certain direction – the director – but no translational order. A nematic liquid crystal cannot support shear stresses, so it is by definition a liquid, but it can support torques, which is the basis for various orientation phenomena relative to external fields. Another kind of liquid crystal is the cholesteric liquid crystal. It can be regarded as a nematic liquid crystal where the director rotates in space around an axis perpendicular to itself – the cholesteric axis or the optical axis. The spatial ro-

tation period or the pitch is of the order of 1 μm or about 500 molecular diameters. A cholesteric liquid crystal is different from its mirror image and it is formed by chiral molecules. It is well-known that the director of liquid crystals can be oriented by the application of an electric or magnetic field, which is utilized in their technological applications. These fields do not do any irreversible work on the system. Once the director has attained the preferred orientation relative to the field, the system will be in thermodynamic equilibrium. On the other hand, dissipative fields such as velocity gradients or temperature gradients do irreversible work on the system [3], so that a thermodynamic equilibrium state cannot be reached. However, it is still possible to reach a steady state, where the director is oriented at a constant angle relative to the field. There is some theoretical and experimental evidence that the

director comes to rest in an orientation where the energy dissipation rate is minimal. This quantity is defined as the irreversible work per unit time and unit volume that is done by dissipative external field on the system and that is converted to heat. More specifically, such orientation phenomena have been observed in simulations of shear flow or planar Couette flow [4, 5] and in experimental measurements of the viscosity [6] in this flow geometry and in simulations of planar elongational flow [7]. In the latter case, it is possible to actually prove that the energy dissipation rate must be either minimal or maximal in a steady state in the linear or Newtonian regime by using the linear phenomenological relations between the velocity gradient and the shear stress. These results can be explained in a more general way by invoking a recently proven theorem stating that the energy dissipation rate is minimal in a steady state in the linear regime [8]. In the case of a nematic liquid crystal subject to a temperature gradient, there are quite a few early experimental works [9–16] that probably imply that the director of a calamitic nematic liquid crystal, *i.e.* a liquid crystal consisting of rod-like molecules, orients perpendicularly to this gradient. This means the heat flow is minimized, since the heat conductivity is minimal in this orientation. Unfortunately, the results of these works are not wholly conclusive because the underlying experiments are very hard to carry out. On the other hand, molecular dynamics simulation of nematic phases of calamitic and discotic soft ellipsoids [17–19] clearly show that they orient perpendicularly and parallel, respectively, to the temperature gradient, so that the heat flow and thereby the energy dissipation rate are minimized. However, one system, where the director definitely orients perpendicularly to the temperature gradient, is the cholesteric liquid crystal, where the cholesteric axis orients parallel to the temperature gradient, so that the director becomes perpendicular to this gradient and the heat flow is minimized [1, 2, 20–22]. This is also in agreement with the above-mentioned dissipation theorem even though the torque orienting the director is proportional to the square of the temperature gradient, whereas it is directly proportional to the velocity gradient in shear flow and elongational flow. However, the temperature gradient is rather weak, so that the relation between this gradient and the heat flow still is linear.

The review is outlined in the following way: in sections II, III and IV molecular dynamics simulation results and experimental measurements on the director orientation and the energy dissipation rate are presented and discussed for shear flow or planar Couette flow, planar elongational flow and heat conduction, respectively. In section V the influence of the thermostat is discussed and in section VI there is a conclusion. The background theory is given in the Appendices.

II. PLANAR COUETTE FLOW

In a laminar planar Couette flow or a shear flow, there is a streaming velocity $\boldsymbol{u}$ in the x-direction, varying linearly in

the z-direction, $u = \gamma z e_x$, where $\gamma = \partial u_x / \partial z$ is the velocity gradient or strain rate, see fig. 1.
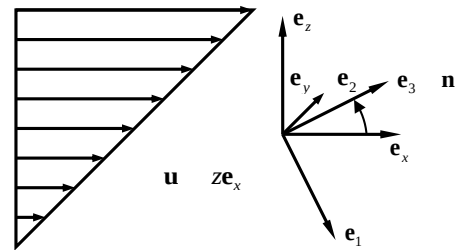

Fig. 1. Planar Couette flow or shear flow arises when there is a streaming velocity in the *x*-direction, varying linearly in the *z*-direction, $\boldsymbol{u} = \gamma z e_x$, where $\gamma = \partial u_x / \partial z$ is the shear rate or velocity gradient. The expression for the relation between the velocity gradient and the pressure tensor becomes simpler by using a director based coordinate system (e_1, e_2, e_3), where the director $\boldsymbol{n}$ points in the e_3-direction, obtained by rotating the ordinary laboratory based coordinate system (e_x, e_y, e_z) with an angle θ around the $e_y = e_2$-axis. Reproduced from reference 3, J. Chem. Phys. **103**, 10378 (1995) with the permission of AIP Publishing

Then it is well-known that the alignment angle, θ, between the director of a nematic liquid crystal and the streamlines is determined by a mechanical stability criterion, namely that the antisymmetric pressure must be zero when no external torques act on the system, *i.e.* that the torques exerted by the vorticity and the strain rate cancel out. This makes it possible to derive a relationship between the alignment angle and the viscosity coefficients in the Newtonian regime by using the linear relation between the pressure tensor and the strain rate, see references [1, 2, 22] and Appendices I and II,

$$\langle p_2^a \rangle = -\tilde{\gamma}_1 \frac{\gamma}{4} - \tilde{\gamma}_2 \frac{\gamma}{4} \cos 2\theta = 0, (1) \qquad (1)$$

where $\tilde{\gamma}_1$ is the twist viscosity, $\tilde{\gamma}_2$ is the cross coupling coefficient between the antisymmetric pressure and the strain rate and $\langle p_2^a \rangle$ is the antisymmetric pressure in the vorticity direction perpendicular to the streamlines and perpendicular to the velocity gradient. The angular brackets denote that the pressure tensor is the ensemble average of a phase function. Then, if $\langle p_2^a \rangle$ is equal to zero, we obtain

$$\cos 2\theta_0 = -\tilde{\gamma}_1 / \tilde{\gamma}_2 (2) \qquad (2)$$

for the preferred alignment angle, θ_0, provided that the ratio $|\tilde{\gamma}_1 / \tilde{\gamma}_2|$ is less than one. Then the liquid crystal is said to be flow stable. This condition is fulfilled in many liquid crystals and θ_0 is between 10 and 20 degrees both in real systems and in simplified coarse grained model systems such as the soft ellipsoid fluid, see references [4–6] and Appendix III. Note, however, that for some systems, often near the nematic-smectic A phase transition, the ratio $|\tilde{\gamma}_1 / \tilde{\gamma}_2|$ is greater than one. This means that there is no orientation angle where the

antisymmetric pressure is zero, so that no steady state is attained. Then the liquid crystal is said to be flow unstable and the director will rotate forever [1, 2, 23, 24]. The problem can be analysed in further detail by considering the algebraic expression for the energy dissipation rate, $\dot{w}_{irr}$, of a flow stable nematic liquid crystal, given by the dyadic product of the symmetric traceless pressure, $\bar{P}$, and the traceless strain rate, $\overline{\nabla u}$,

$$\dot{w}_{irr} = \bar{P} : \overline{\nabla u} = \left(\eta + \frac{\tilde{\eta}_1}{6} + \frac{\tilde{\eta}_3}{2} \sin^2 2\theta + \frac{\tilde{\eta}_2}{2} \cos 2\theta \right) \gamma^2,$$
(3)

where the definitions of the viscosity coefficients η, $\tilde{\eta}_1$, $\tilde{\eta}_2$ and $\tilde{\eta}_3$ and the derivation are given in Appendix II. If the values of the various viscosity coefficients are inserted, it is found that the functional dependence of $\dot{w}_{irr}$ on θ is similar to that given in Fig. 2.
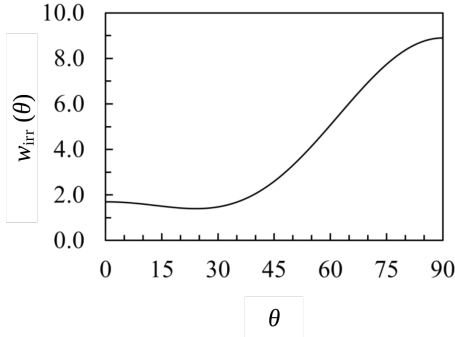

Fig. 2. The energy dissipation rate, $\dot{w}_{irr}$, equation (3), due to the strain rate of a nematic liquid crystal phase of calamitic soft ellipsoids as a function of the director alignment angle, θ, obtained by using the Lagrangian constraint algorithm (A14) to fix the director at various angles relative to the streamlines. The preferred alignment angle attained when no constraints are applied is equal to about 20° which is close to the minimum of $\dot{w}_{irr}$. Reproduced from reference [3], J. Chem. Phys. **103**, 10378 (1995) with the permission of AIP Publishing

This function has been obtained by shear flow simulations using the SLLOD equations of motion [25] for a nematic phase of calamitic soft ellipsoids, see references [4] and [5] and Appendix IVa. The energy dissipation rate is low close to the preferred alignment angle and high when the director is perpendicular to the streamlines and parallel to the velocity gradient. Then, if we study the distribution of the director, we find that it is centered close to the minimum of $\dot{w}_{irr}$. This has also been observed in simulations of shearing nematic phases of discotic soft ellipsoids [5] and when experimentally measured viscosity coefficients are inserted in the equations (2) and (3) and the resulting alignment angle is determined [6]. Thus the system seems to select the alignment angle that minimizes the energy dissipation rate. It could still be argued that the above results are fortuitous. However, there is a recently proven theorem stating that the energy dissipation rate is minimal in a steady state in the linear regime at low fields [8]. As a consequence, the energy dissipation rate (3) must be minimal at the preferred alignment angle, θ_0, given by equation (2). Thus the derivative of the function (3) with respect to θ must be zero for θ_0, giving an additional relation between the viscosity coefficients and the alignment angle,

$$\cos 2\theta_0 - = \frac{\tilde{\eta}_2}{2\tilde{\eta}_3}$$
(4a)

or

$$2\tilde{\eta}_3\tilde{\gamma}_1 + \tilde{\eta}_2\tilde{\gamma}_2 = 0,$$
(4b)

where θ_0 has been eliminated by using equation (2). The expressions (4a) and (2) do not coincide but they must still give the same value of θ_0. This provides an important cross-check for the correctness of the simulation algorithms and experimental methods used to determine the viscosity coefficients and for the computer programs used to run the simulations.

III. PLANAR ELONGATIONAL FLOW

In a planar irrotational elongational flow arising when an incompressible liquid expands in the *x*-direction and contracts in the negative *z*-direction, see Fig. 3, the velocity field and the strain rate are given by $u = \gamma(xe_x - ze_z)$ and $\nabla u = \overline{\nabla u} = \gamma(e_x e_x - e_z e_z)$, respectively. Such a system can be simulated in a continuous manner by using the SLLOD equations of motion [24] together with the Kraynik-Reinelt boundary conditions, see references [25–28], Appendix IVb and fig. 8.
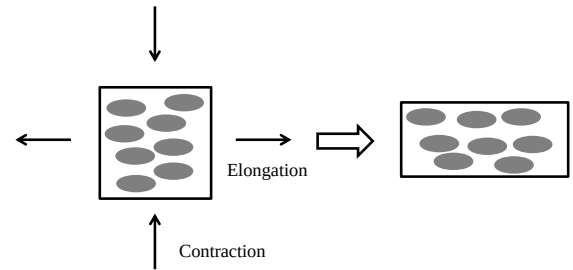

Fig. 3. Schematic representation of a nematic phase of a soft ellipsoid fluid undergoing irrotational extensional flow. The system is elongated in the horizontal direction and contracted in the vertical direction while the volume is constant. The molecules tend to be aligned in the elongation direction

The director alignment angle is in the first place determined by the mechanical stability in same way as in shear flow, which means that the antisymmetric pressure must be zero. In the linear or Newtonian regime, the alignment angle can be found by using the following relation between the antisymmetric pressure and the strain rate, see Appendix II,

$$\langle p_2^a \rangle = -\tilde{\gamma}_2 \frac{\gamma}{2} \sin 2\theta,$$
(5)

where θ denotes the angle between the director and the elongation direction and $\tilde{\gamma}_2$ is the cross coupling coefficient between the antisymmetric pressure and the strain rate. From this expression it is apparent that the alignment angle must be either zero or 90 degrees, *i.e.* where the torque exerted by the strain rate is equal to zero. For a flow stable calamitic nematic liquid crystal the cross coupling coefficient $\tilde{\gamma}_2$ is negative [5], so that the zero degree orientation parallel to the elongation direction is mechanically stable and the 90 degree orientation is unstable. Just as in planar Couette flow or shear flow, a further analysis can be undertaken by considering the algebraic expression for the energy dissipation rate in the linear regime,

$$\dot{w}_{\text{irr}} = \bar{P} : \overline{\nabla u} = \left(4\eta + \frac{2\tilde{\eta}_1}{3} + 2\tilde{\eta}_3 \cos^2 2\theta\right)\gamma^2. \quad (6)$$

If the viscosity coefficient $\tilde{\eta}_3$ is positive this expression is minimal when θ is equal to 45 degrees but this orientation is excluded because of the mechanical stability (5). If $\tilde{\eta}_3$ on the other hand is negative, this expression attains the same minimal value when θ is equal to 0 or 90 degrees, *i.e.* the elongation or contraction direction. Simulations of a nematic phase of calamitic soft ellipsoids have shown that $\tilde{\eta}_3$ is less than zero [7], so that the energy dissipation rate is minimal in the stable orientation also in this case of planar elongational flow. This is in agreement with the dissipation theorem of reference [8]. See also fig. 4 where the angular distribution of the director around the elongation direction is displayed.
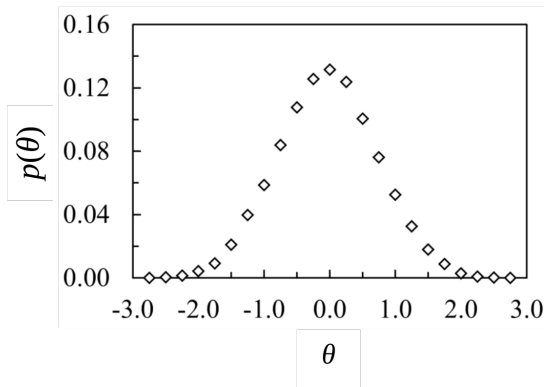

Fig. 4. The angular distribution, $p(\theta)$, of the director of a calamitic nematic liquid crystal consisting of soft ellipsoids around the elongation direction where the angle between the director and the elongation direction is denoted by θ. Reproduced from reference [7], Phys. Chem. Chem. Phys. **17**, 3332 (2015) with permission from the PCCP Owner Societies

IV. HEAT CONDUCTION

The heat flow in an axially symmetric system such as a nematic liquid crystal or a cholesteric liquid crystal is given

by

$$\langle \boldsymbol{J}_Q\rangle = -[\lambda_{\parallel\parallel}\boldsymbol{nn} + \lambda_{\perp\perp}(\boldsymbol{1} - \boldsymbol{nn})]\cdot\frac{\boldsymbol{\nabla} T}{T}, \quad (7)$$

where $\langle \boldsymbol{J}_Q\rangle$ is the heat current density, $\lambda_{\parallel\parallel}$ is the heat conductivity parallel to the director of an ordinary achiral nematic liquid crystal or parallel to the cholesteric axis of a cholesteric liquid crystal and $\lambda_{\perp\perp}$ is the heat conductivity perpendicular to the director of a nematic liquid crystal or perpendicular to the cholesteric axis of a cholesteric liquid crystal, T is the absolute temperature and **n** is the director. Then the energy dissipation rate of the system due to the heat flow becomes

$$\begin{aligned}\dot{w}_{\text{irr}} = &\langle J_Q\rangle\cdot\frac{\boldsymbol{\nabla} T}{T} = \frac{1}{T^2}[\lambda_{\perp\perp}\boldsymbol{\nabla} T\cdot\boldsymbol{\nabla} T \\ &+ (\lambda_{\parallel\parallel} - \lambda_{\perp\perp})(n\cdot\boldsymbol{\nabla} T)^2].\end{aligned} \quad (8)$$

From this expression it follows that $\dot{w}_{\text{irr}}$ depends on the angle between the temperature gradient and the director **n** or between the temperature gradient and the cholesteric axis (since the scalar product of the director and the temperature gradient, $\boldsymbol{n}\cdot\boldsymbol{\nabla} T$, is included). When $\lambda_{\parallel\parallel} > \lambda_{\perp\perp}$, as in a nematic liquid crystal consisting of calamitic molecules, the heat current density and thereby $\dot{w}_{\text{irr}}$ are maximal when the temperature gradient and the director are parallel and minimal when they are perpendicular to each other. Conversely, when $\lambda_{\parallel\parallel} < \lambda_{\perp\perp}$, as in a nematic liquid crystal consisting of discotic molecules, the heat current density and the energy dissipation rate are maximal when the director is perpendicular to the temperature gradient and minimal when it is parallel to the temperature gradient.
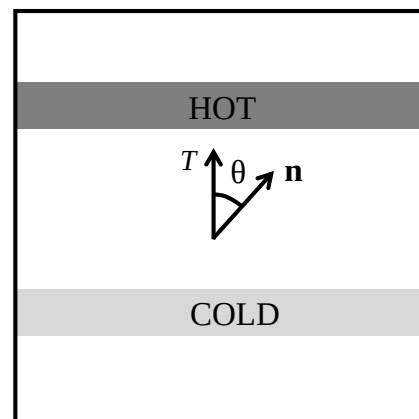

Fig. 5. A temperature gradient is maintained by thermoststatting one region (dark grey) of the system at a high temperature and another region (light grey) at a low temperature whereby heat will flow from the high temperature region to the low temperature region. Reproduced from reference [16], Phys. Chem. Chem. Phys., **16**, 14741 (2014) with permission from the PCCP Owner Societies

The temperature gradient exerts a torque on the molecules around an axis perpendicular to itself and perpendicular to the

director, see fig. 6. Then it is immediately possible to realise that this torque must be zero in the parallel and perpendicular orientations due to symmetry but it is impossible to determine whether these orientations are stable or unstable.
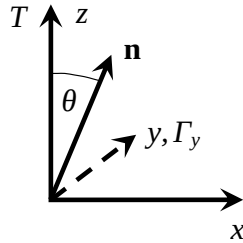

Fig. 6. A schematic view of a nematic liquid crystal subject a temperature gradient is shown. The temperature gradient ∇T points in the z-direction and the director n lies in the *zx*-plane at an angle θ to the *z*-axis. Then a torque Γ arises in the direction of the *y*-axis. Reproduced from reference [16], Phys. Chem. Chem. Phys., **16**, 14741 (2014) with permission from the PCCP Owner Societies

Unfortunately, there is no linear relation between the torque and the temperature gradient since they are pseudovectors and polar vectors, respectively, due to the axial symmetry of the system. However, a quantitative relation between them can be obtained by noting that a cross coupling between a pseudo vector and a symmetric second rank tensor is allowed. The latter quantity can be obtained by forming the dyadic product of the temperature gradient, giving the following relation [17],

$$\Gamma = \mu \varepsilon : nn \cdot \frac{\nabla T}{T}\frac{\nabla T}{T} = \mu n \cdot \frac{\nabla T}{T} n \times \frac{\nabla T}{T} =$$
$$= \mu \left| \frac{\partial_z T}{T} \right|^2 \cos\theta \sin\theta \, e_y = \frac{1}{2}\mu \left| \frac{\partial_z T}{T} \right|^2 \sin 2\theta \, e_y, \tag{9}$$

where Γ is the torque density, μ is a cross coupling coefficient and ε is the Levi-Civita tensor. The third equality is obtained by assuming that the temperature gradient points in the z-direction and the director lies in the *zx*-plane, see fig 6, whereby θ becomes the angle between these two vectors. This relation fulfils the symmetry condition according to which the torque must be zero when the director is parallel or perpendicular to the temperature gradient. Moreover, the torque is proportional to the square of the temperature gradient for given angle θ. Note also that this relation is analogous to that between the strain rate and the antisymmetric pressure in planar elongational flow (5). Unfortunately, it is not possible to derive a Green-Kubo relation for the cross coupling coefficient μ because of the nonlinear relationship.

The director orientation can be determined by simulating systems, where a temperature gradient and a heat flow are maintained by thermostatting different parts of the system at different temperatures, see fig. 5 and reference [17], using the simulation algorithm given in Appendix IVc. Such simulations have shown that the director of nematic liquid crystals

consisting of soft calamitic ellipsoids tends to align perpendicularly to the temperature gradient, see fig. 7, whereas the director of nematic liquid crystals consisting of discotic ellipsoids tends to align parallel to the temperature gradient. Thus the energy dissipation rate is minimal in both cases. Moreover, if the director is constrained to attain a fixed orientation between the perpendicular and parallel orientation relative to temperature gradient by applying a Lagrangian constraint algorithm, the torque exerted can be obtained. Then it is found this torque twists the director of a calamitic system towards the perpendicular orientation and the director of a discotic system towards the parallel orientation. The same orientation behaviour of the directors of calamitic and discotic nematic liquid crystals relative to the temperature gradient was observed in an earlier work [30]. However, then the Evans heat flow algorithm [25] was applied where a fictious external field under non-Newtonian equations of motion rather than a real temperature gradient drives the heat flow. Therefore, it was not possible to determine whether the orientation phenomena were a real effect or a consequence of the non-Newtonian synthetic equations of motion.
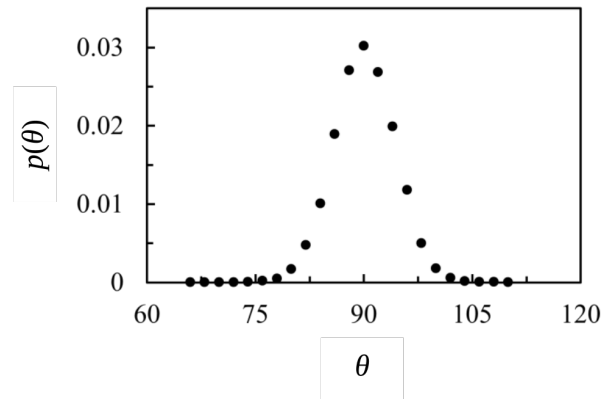

Fig. 7. The angular distribution,$p(\theta)$, of the director of a nematic liquids crystal consisting of soft calamitic ellipsoids around the temperature gradient where the angle between the director and the temperature gradient is denoted by θ. Reproduced from reference [16], Phys. Chem. Chem. Phys., **16**, 14741 (2014) with permission from the PCCP Owner Societies

There are also some early experimental works on the orientation of the director of nematic liquid crystals relative to temperature gradients [9–16] that probably support the conclusions of these heat flow simulations. Unfortunately, it is very difficult to carry out these experiments because if the temperature gradient is too large, there will be convection in the system and if the temperature gradient is too small, it will not be strong enough to overcome the elastic torques or surface torques. Therefore, these experiments are not fully conclusive.

Finally, one example where the director orientation relative to a temperature gradient definitely is the one that min-

imises the energy dissipation rate is a cholesteric liquid crystal. In this system the director rotates in space around the cholesteric axis forming a spiral structure. Then experimental studies, where a temperature gradient is applied, have shown that the cholesteric axis orients parallel to the temperature gradient, whereby the energy dissipation rate is minimised since the heat conductivity is greater in the direction perpendicular to the cholesteric axis than in the parallel direction. Moreover, the whole spiral structure starts rotating in time. This phenomenon is known as thermomechanical coupling [1, 2, 20–22, 31, 32]. There are quite a few experimental studies available on this phenomenon, where it has been found in a conclusive way that the cholesteric axis remains parallel to the temperature gradient, so this orientation seems to be stable and thus the energy dissipation rate is minimal. We can consequently conclude that the orientation of the director relative to the temperature gradient is consistent with the dissipation theorem of reference [8] even though the coupling between the torque and the temperature gradient is quadratic rather than linear and the system is inhomogeneous. However, the temperature gradient is rather weak, so we still remain in the linear regime.

V. EFFECTS OF THE THERMOSTAT

In the above simulations of shear flow and elongational flow the velocity gradient does work on the system that is converted to heat, which must be removed in order to keep the temperature constant and to maintain a steady state. In a real macroscopic system this takes place by heat conduction to the system boundaries and this could in principle be arranged in a microscopic simulation cell as well. Unfortunately, this is inconvenient because a temperature gradient of molecular dimensions would make the system inhomogeneous and thus make it difficult to define the thermodynamic state. Therefore, the temperature is kept constant by forcing the kinetic energy to be a constant of motion by applying a Gaussian thermostat, see equation (A11). This thermostat was originally devised independently by Hoover *et al.* [33–35] and by Evans [25]. The equilibrium ensemble averages of the phase functions and time correlation functions generated when this thermostat is used are essentially canonical [36]. Away from equilibrium, it can be shown that the effect of the Gaussian thermostat on the ensemble averages is proportional to the square of the external field whereas the thermodynamic fluxes driven by the field are directly proportional to the field in a linear transport process. Thus the corresponding linear transport coefficients that are equal to the ratio of the flux and the field in the limit of zero field are independent of the thermostat. Therefore, transport coefficients obtained from the simulations of shear flow and elongational flow are independent of the thermostat since there is a linear relation between the velocity gradient and the shear stress in the Newtonian regime and since we are interested in the limit of zero velocity gradient.

The situation is different in the heat flow simulations because here we actually want a temperature gradient. This gradient is obtained by applying two bar thermostats at different temperatures acting over a limited range and separated by a distance that is long compared to this range, see fig. 5 and equation (A.13). Therefore, the movements of only a small fraction of the molecules are affected by the thermostats, whereas the movements of the majority of the molecules away from the bar thermostats are governed by the ordinary Newtonian equations of motion. Thus it is reasonable to assume that the influence of the details of the thermostat on the ensemble averages of the phase functions is limited in this case, too.

VI. CONCLUSION

We have reviewed molecular dynamics simulations and experimental work on director orientation phenomena in nematic liquid crystals and in cholesteric liquid crystals under external dissipative fields such as velocity gradients and temperature gradients. In all the examples the liquid crystals seems to attain precisely that alignment angle relative to the external dissipative field that minimises the energy dissipation rate.

In a nematic liquid crystal the director orientation is in the first place determined by a mechanical stability criterion, namely that the external torques acting on the system must be zero at mechanical equilibrium. This makes it possible to derive an exact relation between the alignment angle relative to the streamlines and the viscosity coefficients in the linear or Newtonian regime of planar elongational flow and of planar Couette flow. It can be shown that the elongation direction is the stable orientation of flow stable calamitic nematic liquid crystals undergoing elongational flow in the linear regime. It can also be shown that the value of the energy dissipation rate is the same in the contraction direction and in the elongation direction and that this value is either the maximal or the minimal value by using the linear phenomenological relations between the strain rate and the pressure. Simulations of the calamitic soft ellipsoid fluid have shown that the energy dissipation rate is minimal in the elongation direction. In planar Couette flow both simulations and experiments imply that the energy dissipation rate is minimal at the mechanically stable orientation. In contrast to elongational flow, this does not follow from the linear relation between pressure and the strain rate.

It is possible to think that these observations are special cases. However, they follow from a recently proven theorem stating that the energy dissipation rate is minimal in a steady state in the linear regime. Thus the energy dissipation rate must be minimal at the alignment angle given by the mechanical stability criterion. This is in fact an important consistency condition for the experimental methods and the simulations algorithms used to evaluate the various viscosity

coefficients and for the programme codes used to carry out the simulations.

In calamitic nematic liquid crystals, the heat conductivity is larger in the direction parallel to the director than in the perpendicular direction and the reverse is true for discotic nematic liquid crystals. Thus the energy dissipation rate due to the heat flow depends on the angle between the director and the temperature gradient. When a nematic liquid crystal is subjected to a temperature gradient a torque is exerted on the molecules. Due to symmetry, this torque must be proportional to the square of the temperature gradient and it must be zero when the director is parallel or perpendicular to this gradient.

In simulations of nematic phases of soft ellipsoids under a temperature gradient it turns out that the director of a calamitic nematic liquid crystal aligns perpendicularly to the temperature gradient whereas the director of a discotic nematic liquid crystal orients parallel to this gradient. In both cases the energy dissipation rate is minimal. These simulation results are probably supported by some experimental measurements but they are difficult to carry out in practice so they are not fully conclusive.

Finally, one system where there definitely is conclusive experimental evidence for the fact that the director attains the orientation that minimises the energy dissipation rate due to a temperature gradient is the cholesteric liquid crystal. The cholesteric axis of droplets of cholesteric liquid crystals orient parallel to a temperature gradient and the director rotates. This is a well-established phenomenon observed in studies of thermomechanical coupling and since the heat conductivity is lower in the direction of the cholesteric axis than in the perpendicular direction the energy dissipation rate is minimal in this case.

Thus the director orientation relative to a temperature gradient also follows the dissipation theorem even though there is a quadratic coupling between the torque and the temperature gradient. However, the temperature gradients are rather low so we are still in the linear regime.

Acknowledgement

APPENDIX I. ORDER PARAMETER, DIRECTOR AND DIRECTOR ANGULAR VELOCITY

In order to describe transport properties of a liquid crystal we must first define the order parameter, the director and the

director angular velocity. In an axially symmetric system such as a nematic or a smectic A liquid crystal the order parameter, S, is given by the largest eigenvalue of the order tensor,

$$\boldsymbol{Q} = \frac{3}{2}\left(\frac{1}{N}\sum_{i=1}^{N} \hat{\boldsymbol{u}}_i \hat{\boldsymbol{u}}_i - \frac{1}{3}\boldsymbol{1} \right), \qquad (A.1)$$

where N is the number of particles, $\{\hat{\boldsymbol{u}}_i; \ 1 \leq i \leq N\}$ is some characteristic vector of the molecule, in the case of bodies of revolution it can be taken to be parallel to the axis of revolution, but in a more realistic all atom model some other vector in the molecule has to be defined as $\hat{\boldsymbol{u}}_i$, and $\boldsymbol{1}$ is the unit second rank tensor. When the molecules are perfectly aligned in the same direction, the order parameter is equal to unity, and when the orientation is completely random, it is equal to zero. The eigenvector corresponding to the order parameter is defined as the director, $\boldsymbol{n}$, and it is a measure of the average orientation of the molecules in the system. The order tensor can also be expressed as

$$\boldsymbol{Q} = \frac{3}{2}S\left(nn - \frac{1}{3}\boldsymbol{1} \right). \qquad (A.2)$$

The director angular velocity is given by $\boldsymbol{\Omega} = \boldsymbol{n} \times \dot{\boldsymbol{n}}$. In a macroscopic system the order tensor and the order parameter are functions of the position in space but in a small system such as a simulation cell with dimensions of the order of some ten molecular lengths there is only one director and one order parameter for the whole system.

APPENDIX II. RELATION BETWEEN THE PRESSURE TENSOR, VELOCITY GRADIENT AND VISCOSITY COEFFICIENTS

The relation between the velocity gradient, $\boldsymbol{\nabla u}$, and the pressure tensor, $\boldsymbol{P}$, is more complicated in an axially symmetric system such as nematic liquid crystal than in an isotropic fluid due to the lower symmetry. In order to derive the linear phenomenological relations between the velocity gradient and the pressure it is appropriate to begin by identifying the thermodynamic forces and fluxes in the expression for the irreversible entropy production [3, 4, 23, 37]:

$$\sigma = -\frac{1}{T}\left\{ \overline{\boldsymbol{P}} : \overline{\boldsymbol{\nabla u}} + 2P^a \cdot (\frac{1}{2}\boldsymbol{\nabla} \times \boldsymbol{u} - \boldsymbol{\Omega}) \right.$$
$$\left. + \left(\frac{1}{3}\mathrm{Tr}(\boldsymbol{P}) - p_{eq} \right)\boldsymbol{\nabla} \cdot \boldsymbol{u} \right\}, \qquad (A.3)$$

where T is the absolute temperature, and $\boldsymbol{u}$ is the streaming velocity. The various parts of the second rank tensor are denoted in the following manner: the symmetric traceless

part is given by $\overline{A} = \frac{1}{2}(A + A^T) - (1/3)\mathrm{Tr}(A)\mathbf{1}$ and the pseudovector dual of the antisymmetric part is denoted by $A^a = -\frac{1}{2}\varepsilon : A = -\frac{1}{2}\varepsilon_{\alpha\beta\gamma}A_{\gamma\beta}$, where ε is the Levi-Civita tensor. Three pairs of thermodynamic forces and fluxes can be identified by inspection of the irreversible entropy production, namely the symmetric traceless pressure tensor and the traceless strain rate, $\overline{P}$ and $\overline{\nabla u}$, the antisymmetric pressure and the difference between the vorticity and the director angular velocity, P^a and $\frac{1}{2}\nabla \times u - \Omega$, and the difference between the trace of the pressure tensor and the equilibrium pressure of a quiescent liquid crystal, and the trace of the strain rate, $(1/3)\mathrm{Tr}(P) - p_{eq}$ and $\nabla \cdot u$. Note that that the strain rate is defined as $\frac{1}{2}[\nabla u + (\nabla u)^T]$ and it is always symmetric. In a uniaxially symmetric nematic liquid crystal the relations between the pressure and the velocity gradient can be deduced by symmetry arguments and they can be expressed in a few different equivalent ways [23, 37]. It has been found that a notation due to Hess [37] is the most convenient one for deducing Green-Kubo relations and NEMD-algorithms:

$$\langle \overline{P} \rangle = - 2\eta\overline{\nabla u} - \tilde{\eta}_1 \overline{nn \cdot \nabla u} - 2\tilde{\eta}_3\overline{nn} \; \overline{nn} : \overline{\nabla u}$$
$$+2\tilde{\eta}_2\overline{nn \cdot \varepsilon \cdot (\frac{1}{2}\nabla \times u - \Omega)} - \zeta\overline{nn} \, \nabla \cdot u, \tag{A.4a}$$

$$\langle P^a \rangle = -\frac{\tilde{\gamma}_1}{2}(\frac{1}{2}\nabla \times u - \Omega) - \frac{\tilde{\gamma}_2}{2}\varepsilon : (\overline{nn} \cdot \overline{\nabla u}) \tag{A.4b}$$

and

$$\frac{1}{3}\langle \mathrm{Tr}(P) \rangle - p_{eq} = -\eta_V \nabla \cdot u - \kappa \overline{nn} : \overline{\nabla u}, \tag{A.4c}$$

where the products involving the Levi-Civita tensor ε are defined in the following way: $\varepsilon : A = \varepsilon_{\alpha\beta\gamma}A_{\gamma\beta}$ and $A \cdot \varepsilon \cdot B = A_{\alpha\beta}\varepsilon_{\beta\gamma\delta}B_\delta$. The quantities η, $\tilde{\eta}_1$ and $\tilde{\eta}_3$ are shear viscosities, $\tilde{\gamma}_1$ is the twist viscosity, η_V is the volume viscosity, $\tilde{\eta}_2$ is the cross coupling coefficient between the difference between the vorticity and the director angular velocity, and the symmetric traceless pressure. According to the Onsager reciprocity relations (ORR) this coefficient is equal to $\tilde{\gamma}_2/2$, the cross coupling coefficient between the traceless strain rate and the antisymmetric pressure. The trace of the strain rate and the symmetric traceless pressure are related by the cross-coupling coefficient ζ, which, according to the ORR, is equal to the cross-coupling coefficient κ between the traceless strain rate and the difference between the trace of the pressure tensor and the equilibrium pressure.

Application of a planar Couette velocity gradient, $\nabla u = \gamma e_z e_x$, where $\gamma = \partial_z u_x$ is the shear rate, and fixation of the director in the zx-plane at an angle θ relative to the stream lines, see fig. 1, by application of an electric or a magnetic field gives the following relations between the pressure tensor

components and the strain rate in a director based coordinate system (e_1, e_2, e_3) where the director points in the e_3-direction:

$$\langle \bar{p}_{11} \rangle = \left(\eta + \frac{\tilde{\eta}_3}{3}\right)\gamma \sin 2\theta, \tag{A.5a}$$

$$\langle \bar{p}_{22} \rangle = \frac{1}{3}(\tilde{\eta}_1 + \tilde{\eta}_3)\gamma \sin 2\theta, \tag{A.5b}$$

$$\langle \bar{p}_{33} \rangle = -\left(\eta + \frac{\tilde{\eta}_1}{3} + \frac{2\tilde{\eta}_3}{3}\right)\gamma \sin 2\theta, \tag{A.5c}$$

$$\langle \bar{p}_{31} \rangle = \left(\eta + \frac{\tilde{\eta}_1}{6}\right)\gamma \cos 2\theta + \tilde{\eta}_2\frac{\gamma}{2} \tag{A.5d}$$

and

$$2\langle p_2^a \rangle = \langle \hat{\lambda}_2 \rangle = -\tilde{\gamma}_1\frac{\gamma}{2} - \tilde{\gamma}_2\frac{\gamma}{2}\cos 2\theta, \tag{A.5e}$$

where $\hat{\lambda}_2$ is the external torque density acting on the system. From these equations it is apparent that the various elements of the pressure tensor are linear functions of $\sin 2\theta$ and $\cos 2\theta$, so the various viscosity coefficients can be evaluated by fixing the director at a few different angles relative to the stream lines and calculating the averages of the pressure tensor elements.

In a planar elongational flow [7, 27–29], where the elongation direction is parallel to the x-axis and the contraction direction is parallel to the negative z-axis, the velocity field is equal to $u = \gamma(xe_x - ze_z)$, so that the velocity gradient becomes $\nabla u = \gamma(e_x e_x - e_z e_z)$ where $\gamma = \partial_x u_x = -\partial_z u_z$. Then the linear relations between the velocity gradient and the pressure become the following in a director based coordinate system (e_1, e_2, e_3) where the director points in the e_1-direction and θ is the angle between the director and the elongation direction or x-axis, $e_2 = e_y$ and $e_3 = e_1 \times e_2$,

$$\langle \bar{p}_{11} \rangle = -2\left(\eta + \frac{\tilde{\eta}_3}{3}\right)\gamma \cos 2\theta, \tag{A.6a}$$

$$\langle \bar{p}_{22} \rangle = -\frac{2}{3}(\tilde{\eta}_1 + \tilde{\eta}_3)\gamma \cos 2\theta, \quad (A.6b) \tag{10}$$

$$\langle \bar{p}_{33} \rangle = 2\left(\eta + \frac{\tilde{\eta}_1}{3} + \frac{2\tilde{\eta}_3}{3}\right)\gamma \cos 2\theta, \tag{A.6c}$$

$$\langle \bar{p}_{31} \rangle = \left(2\eta + \frac{\tilde{\eta}_1}{3}\right)\gamma \sin 2\theta \tag{A.6d}$$

and

$$2\langle p_2^a \rangle = \langle \hat{\lambda}_2 \rangle = -\tilde{\gamma}_2 \gamma \sin 2\theta. \tag{A.6e}$$

If these expressions for the pressure tensor are inserted in the expression for energy dissipation rate (A3) we obtain

$$\dot{w}_{\text{irr}} = \overline{\boldsymbol{P}} : \overline{\boldsymbol{\nabla} \boldsymbol{u}} = -\left\langle \frac{1}{2}(\bar{p}_{33}^s - \bar{p}_{11}^s) \sin 2\theta - \bar{p}_{31}^s \cos 2\theta \right\rangle_\gamma \gamma$$

$$= \left(\eta + \frac{\tilde{\eta}_1}{6} + \frac{\tilde{\eta}_3}{2} \sin^2 2\theta + \frac{\tilde{\eta}_2}{2} \cos 2\theta \right) \gamma^2 \tag{A.7}$$

for planar Couette flow and

$$\dot{w}_{\text{irr}} = \left(4\eta + \frac{2\tilde{\eta}_1}{3} + 2\tilde{\eta}_3 \sin^2 2\theta \right) \gamma^2 \tag{A.8}$$

for planar elongational flow. The subscript γ denotes that the average is evaluated in a nonequilibrium ensemble at a finite shear rate.

APPENDIX III. THE GAY-BERNE POTENTIAL

In order to evaluate the above expressions for the irreversible work in shear flow, elongational flow and heat flow, we have simulated a coarse grained model system composed of molecules interacting via a purely repulsive version of the commonly used Gay-Berne potential [18, 19, 30].

$$U(\boldsymbol{r}_{12}, \hat{\boldsymbol{u}}_1, \hat{\boldsymbol{u}}_2) =$$

$$= 4\varepsilon(\hat{\boldsymbol{r}}_{12}, \hat{\boldsymbol{u}}_1, \hat{\boldsymbol{u}}_2) \left(\frac{\sigma_0}{r_{12} - \sigma(\hat{\boldsymbol{r}}_{12}, \hat{\boldsymbol{u}}_1, \hat{\boldsymbol{u}}_2) + \sigma_0} \right)^{18}, \tag{A.9}$$

where $\boldsymbol{r}_{12} = \boldsymbol{r}_2 - \boldsymbol{r}_1$ is the distance vector from the centre of mass of molecule 1 to the centre of mass of molecule 2, $\hat{\boldsymbol{r}}_{12}$ is the unit vector in the direction of $\boldsymbol{r}_{12}$, r_{12} is the length of the vector $\boldsymbol{r}_{12}$ and $\hat{\boldsymbol{u}}_1$ and $\hat{\boldsymbol{u}}_2$ are parallel to the axes of revolution of molecule 1 and molecule 2. The parameter σ_0 is the length of the axis perpendicular to the axis of revolution, *i.e.* the minor axis of a calamitic ellipsoid of revolution and the major axis of a discotic ellipsoid of revolution. The strength and range parameters are given by

$$\varepsilon(\hat{\boldsymbol{r}}_{12}, \hat{\boldsymbol{u}}_1, \hat{\boldsymbol{u}}_2) = \varepsilon_0 \left[1 - \chi^2 (\hat{\boldsymbol{u}}_1 \cdot \hat{\boldsymbol{u}}_2)^2 \right]^{-1/2}$$

$$\times \left\{ 1 - \frac{\chi'}{2} \left[\frac{(\hat{\boldsymbol{r}}_{12} \cdot \hat{\boldsymbol{u}}_1 + \hat{\boldsymbol{r}}_{12} \cdot \hat{\boldsymbol{u}}_2)^2}{1 + \chi' \hat{\boldsymbol{u}}_1 \cdot \hat{\boldsymbol{u}}_2} \right. \right.$$

$$\left. \left. + \frac{(\hat{\boldsymbol{r}}_{12} \cdot \hat{\boldsymbol{u}}_1 - \hat{\boldsymbol{r}}_{12} \cdot \hat{\boldsymbol{u}}_2)^2}{1 - \chi' \hat{\boldsymbol{u}}_1 \cdot \hat{\boldsymbol{u}}_2} \right] \right\}^2 \tag{A.10a}$$

and

$$\sigma(\hat{\boldsymbol{r}}_{12}, \hat{\boldsymbol{u}}_1, \hat{\boldsymbol{u}}_2) = \sigma_0 \left\{ 1 - \frac{\chi}{2} \left[\frac{(\hat{\boldsymbol{r}}_{12} \cdot \hat{\boldsymbol{u}}_1 + \hat{\boldsymbol{r}}_{12} \cdot \hat{\boldsymbol{u}}_2)^2}{1 + \chi \hat{\boldsymbol{u}}_1 \cdot \hat{\boldsymbol{u}}_2} \right. \right.$$

$$\left. \left. + \frac{(\hat{\boldsymbol{r}}_{12} \cdot \hat{\boldsymbol{u}}_1 - \hat{\boldsymbol{r}}_{12} \cdot \hat{\boldsymbol{u}}_2)^2}{1 - \chi \hat{\boldsymbol{u}}_1 \cdot \hat{\boldsymbol{u}}_2} \right]^{-1/2} \right\}, \tag{A.10b}$$

where the parameter χ is equal to $(\kappa^2 - 1)/(\kappa^2 + 1)$ and κ is the ratio of the axis of revolution and the axis perpendicular to this axis, χ' is equal to $(\kappa'^{1/2} - 1)/(\kappa'^{1/2} + 1)$ and κ' is the ratio of the potential energy minima of the side by side and end to end configurations of calamitic ellipsoids or the ratio of the edge-to-edge and face-to-face configurations of discotic ellipsoids, and ε_0 denotes the depth of the potential minimum in the cross configuration, where $\hat{\boldsymbol{r}}_{12}$, $\hat{\boldsymbol{u}}_1$ and $\hat{\boldsymbol{u}}_2$ are perpendicular to each other. The parameters κ and κ' have been given the values 3 and 5, respectively, for the calamitic ellipsoids and 1/3 and 1/5 for the discotic ellipsoids. Note that the potential is purely repulsive, so there are no potential minima but the value of κ' optimised for the attractive Gay-Berne potential has been retained. The transport properties of this system of purely repulsive soft ellipsoids are similar to those of a system where the molecules interact according to the conventional Gay-Berne potential with attraction as well, so the results are still relevant.

APPENDIX IV. EQUATIONS OF MOTION

A. Shear flow or planar Couette flow

In order to study shear flow and to calculate the viscosity and director alignment angles relative to the streamlines, it is convenient to apply the SLLOD equations of motion [25]. In linear space they take the following form:

$$\dot{\boldsymbol{r}}_i = \frac{\boldsymbol{p}_i}{m} + \gamma \boldsymbol{r}_{zi} \boldsymbol{e}_x \tag{A.11a}$$

and

$$\dot{\boldsymbol{p}}_i = \boldsymbol{F}_i - \gamma p_{zi} \boldsymbol{e}_x - \xi \boldsymbol{p}_i, \tag{A.11b}$$

where $\boldsymbol{r}_i$ and $\boldsymbol{p}_i$ are the position and peculiar momentum, *i.e.* the momentum relative to the streaming velocity, of molecule i, m is the molecular mass, $\gamma = \partial u_x / \partial z$ is the shear rate, *i. e.* there is a streaming velocity u_x in the x-direction varying linearly in the z-direction, e_x is the unit vector in the x-direction, $\boldsymbol{F}_i$ is the force exerted on molecule i by the other molecules and ξ is a Gaussian thermostatting multiplier given by the constraint that the linear peculiar kinetic energy should be a constant of motion,

$$\xi = \frac{\sum_{i=1}^{N} \left[\boldsymbol{F}_i \cdot \boldsymbol{p}_i - \gamma p_{ix} p_{iz} \right]}{\sum_{i=1}^{N} \boldsymbol{p}_i^2}. \tag{A.11c}$$

B. Elongational flow

The SLLOD equations of motion can also be applied to planar elongational flow. Then a problem is that, if the simulation cell is elongated in the *x*-direction and contracted in the *z*-direction, the simulation can only continue until the width in the *z*-direction is equal to twice the range of the interaction potential. However, if the angle between the elongation direction and the *x*-axis is set to an angle, φ, the periodic lattice of originally quadratic simulation cells is gradually deformed to a lattice of cells shaped like parallelograms. Then it can be shown that for a special value of this angle, φ_0, the lattice of parallelograms can be remapped onto the original quadratic lattice after a certain time period, so that the simulation becomes continuous, see fig. 8 and references [7] and [26–29] for details.
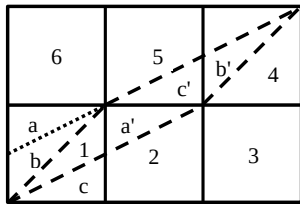

Fig. 8. The Kraynik-Reinelt boundary conditions. The original simulation cell is square 1. When the angle between the elongation direction and the horizontal direction is equal to φ_0, square 1 is deformed to a parallelogram, which, after a given time interval, becomes the dashed parallelogram, partially covering the squares (1–6). Then the triangles a', b' and c' in the parallelogram are periodic copies of the triangles a, b and c in square 1. If the primed triangles are moved to the corresponding unprimed triangles, a square is recovered and the simulation can proceed. Reproduced from reference [7], Phys. Chem. Chem. Phys. **17**, 3332 (2015) with permission from the PCCP Owner Societies

Then, if the angle between the elongation direction and the *x*-axis is equal to φ_0 the velocity gradient becomes $\nabla u = \gamma(e'_x e'_x - e'_z e'_z)$, where $e'_x = e_x \cos\varphi_0 - e_z \sin\varphi_0$ and $e'_z = e_x \sin\varphi_0 + e_y \cos\varphi_0$ are the elongation and contraction directions. Inserting this gradient in the SLLOD equations of motion gives,

$$\dot{r}_i = \frac{p_i}{m} + r_i \cdot \nabla u = \frac{p_i}{m} + \gamma r_i \cdot (e'_x e'_x - e'_z e'_z) \quad \text{(A.12a)}$$

and

$$\begin{aligned} \dot{p}_i =& F_i - p_i \cdot \nabla u - \beta = F_i \\ & - \gamma p_i \cdot (e'_x e'_x - e'_z e'_z) - \xi p_i - \beta, \end{aligned} \quad \text{(A.12b)}$$

where r_i and p_i are the position and peculiar momentum of molecule *i*, F_i is the force exerted on molecule *i* by the other molecules, *m* is the molecular mass, *u* is the streaming velocity, γ is the strain rate and β is a constraint multiplier used to conserve the linear momentum.

C. Heat flow algorithm

A temperature gradient can be established by keeping different regions, 1 and 2, of a system at different temperatures, see fig. 5, by using variant of an algorithm originally due to Ikeshoji and Hafskjold [38],

$$\begin{aligned} m\ddot{r}_i =& F_i - \alpha_1 m \left(w_{1i}\dot{r}_i - \frac{1}{N}\sum_{j=1}^{N} w_{1j}\dot{r}_j \right) \\ & - \alpha_2 m \left(w_{2i}\dot{r}_i - \frac{1}{N}\sum_{j=1}^{N} w_{2j}\dot{r}_j \right), \end{aligned} \quad \text{(A.13)}$$

where *m* is the molecular mass, $\dot{r}_i$ is the velocity of molecule *i*, F_i is the force exerted on molecule *i* by the other molecules, *N* is the number of molecules, α_1 and α_2 are the thermostatting multipliers for region 1 and 2, respectively, and w_{1i} and w_{2i} are two normalized weight functions for these regions. The algebraic expressions for the thermostatting multipliers are determined by requiring that the rate of change of the kinetic energy should be a constant of motion, see reference [17] for details. It is convenient to let these two weight functions be Gaussian functions centered in the two regions and with decay lengths that are considerably shorter than the distance between the two regions, so that the thermostats can be regarded as a bar heater and a bar cooler. In this way the constraints do not interfere with each other and only the molecules in the rather narrow thermostatted regions are affected by the thermostat, whereas the other molecules move according to the ordinary Newtonian equations of motion.

D. Director constraint algorithm

Since the molecules studied in the molecular dynamics simulation works that are reviewed in this article are rigid, the Euler equations are applied in angular space. Moreover, since the purpose often is to find the stable orientations of the director relative to an external dissipative field, it is interesting to calculate the torque exerted on the liquid crystal, when the director attains various fixed angles relative to this field. This can be done by adding Lagrangian constraints to the Euler equations [30],

$$I\dot{\omega}_i = \Gamma_i + \lambda_x \frac{\partial\Omega_x}{\partial\omega_i} + \lambda_y \frac{\partial\Omega_y}{\partial\omega_i}, \quad \text{(A.14)}$$

where *I* is the moment of inertia around the axes perpendicular to the axis of revolution, ω_i is the angular velocity of molecule *i*, Γ_i is the torque exerted on molecule *i* by the other molecules, Ω_x and Ω_y are the *x*- and *y*-components of the director angular velocity, and λ_x and λ_y are Lagrangian constraint multipliers keeping the *x*- and *y*-components of the director angular acceleration equal to zero. These multipliers are determined in such a way that the director angular

acceleration becomes a constant of motion. Then if the initial director angular acceleration and angular velocity are equal to zero, the director will remain fixed in space for all subsequent times and the time averages of the constraint multipliers will be equal to the torque exerted on the director by the external field.

References

[1] S. Chandrasekhar, *Liquid Crystals*, Cambridge University Press, Cambridge, 1992.

[2] P.G. de Gennes and J. Prost, *The Physics of Liquid Crystals*, Clarendon Press, Oxford, 1993.

[3] S.R. de Groot and P. Mazur, *Nonequilibrium Thermodynamics*, Dover, New York, 1984.

[4] S. Sarman, J. Chem. Phys., **103**, 393 (1995)

[5] S. Sarman, J. Chem. Phys., **103**, 10378 (1995)

[6] J. Jadzyn and G. Czechowski, J. Phys.: Condens. Matter, **13**, L261 (2001)

[7] S. Sarman and A. Laaksonen, Phys. Chem. Chem. Phys. **17**, 3332 (2015)

[8] D.J. Evans, D.J. Searles and S.R. Williams, *Fundamentals of Classical Statistical Thermodynamics: Dissipation, Relaxation and Fluctuation Theorems*, Wiley-VCH (2016)

[9] G.W. Stewart, J. Chem. Phys., **4**, 231 (1936)

[10] D.O. Holland and G.W. Stewart, Phys. Rev., **51**, 62 (1937)

[11] G.W. Stewart, D.O. Holland and L.M. Reynolds, Phys. Rev., **58**, 174 (1940)

[12] G.W. Stewart, Phys. Rev., **69**, 51 (1946).

[13] J.J.C. Picot and A.G. Fredrickson, Ind. Eng. Chem. Fundam., **1**, 84 (1968)

[14] J. Fisher and A.G. Fredrickson, Mol. Cryst. Liq. Cryst., **6**, 255 (1969)

[15] M.N. Patharkar, V.S.V. Rajan and J.J.C. Picot, Mol. Cryst. Liq. Cryst., **15**, 225 (1971)

[16] P.K. Currie, Rheol. Acta, **12**, 165 (1973)

[17] S. Sarman and A. Laaksonen, Phys. Chem. Chem. Phys., **16**, 14741 (2014)

[18] J.G. Gay and B.J. Berne, J. Chem. Phys., **74**, 3316 (1981)

[19] M.A. Bates and G.R. Luckhurst, J. Chem. Phys., **104**, 6696 (1996)

[20] N. Éber and I. Jánossy, Mol. Cryst. Liq. Cryst., Lett. Sect., **72**, 233 (1982)

[21] P. Oswald and A. Dequidt, Phys. Rev. Lett., **100**, 217802 (2008)

[22] P. Oswald, Eur. Phys. J. E: Soft Matter Biol. Phys., **35**, 10 (2012)

[23] F.M. Leslie, Quart. Journ. Mech. Appl. Math. **19**, 357 (1966)

[24] S. Sarman and A. Laaksonen, J. Chem. Phys., **131**, 144904 (2009)

[25] D.J. Evans and G.P. Morriss, *Statistical Mechanics of Nonequilibrium Liquids*, Academic Press, London, 1990.

[26] A.M. Kraynik and D.A. Reinelt, Int. J. Multiphase Flow, **18**, 1045 (1992)

[27] A. Baranyai and P.T. Cummings, J. Chem. Phys., **103**, 10217 (1995)

[28] B.D. Todd and P.J. Daivis, Phys. Rev. Lett., **81**, 1118 (1998)

[29] B.D. Todd and P.J. Daivis, Molecular Simulation, **33**, 189 (2007)

[30] S. Sarman, J. Chem. Phys., **101**, 480 (1994)

[31] F.M. Leslie, Proc. R. Soc. A, **A307**, 359 (1968)

[32] F.M. Leslie, Symp. Faraday Soc., **5**, 33 (1971)

[33] W.G. Hoover, A.J.C. Ladd and B. Moran, Phys. Rev. Lett., **48**, 1818 (1982)

[34] D.J. Evans, W.G. Hoover, B.H. Failor, B. Moran and A.J.C. Ladd, Phys. Rev. A, **28**, 1016 (1983)

[35] W.G. Hoover, *Computational Statistical Mechanics*, Elsevier (1991)

[36] D.J. Evans and S. Sarman, Phys. Rev. E, **48**, 65 (1992)

[37] S. Hess, J. Non-Equilib. Thermodyn. **11**, 175 (1986)

[38] T. Ikeshoji and B. Hafskjold, Molecular Physics, **81**, 251(1994)

Sten Sarman received his PhD in physical chemistry at the Royal Institute of Technology in Stockholm, Sweden in 1990 under the supervision of Professor Roland Kjellander. After this he became a postdoctoral fellow at the Australian National University under Professor Denis Evans. In 1994 he went back to Sweden to the department of physical chemistry at Göteborg University in Göteborg, Sweden. His main research interests are various aspects of liquid state chemical physics such as integral equation theory of inhomogeneous liquids and molecular dynamics simulation of complex liquids such as liquid crystals and ionic liquids.

Yong-Lei Wang received his PhD in Physical Chemistry in 2013 from Stockholm University, Sweden, under Prof. A. Laaksonen and Prof. Z-Y. Lu (Jilin University, China). Subsequently, he was a postdoctoral researcher at Stockholm University working with Prof. A. Laaksonen, and at KTH Royal Institute of Technology with Prof. L. Kloo (chemistry) and Prof. S. Glavatskih (Mechanics). Since Sept. 2016 he works as a Wallenberg Postdoctoral Fellow with Prof. M. Fayer at Stanford University. His work has been focused on the development and application of computational techniques for studying liquid crystals, polyelectrolytes, and ionic liquid.

Aatto Laaksonen is a Professor in Physical Chemistry at Stockholm University; BSc Mathematics, Stockholm University; PhD in Physical Chemistry Stockholm University 1981; Postdoctoral research with Dr. Victor Saunders 1982, Daresbury Laboratory, UK; Postdoctoral research with Dr. Enrico Clementi 1983–1985, IBM research laboratories in Poughkeepsie and in Kingston, USA. Active in the area of computational materials science, being responsible of modelling work to design new nano- and mesoporous materials for separation and storage of gases and for heterogeneous catalysis processes inside the pores within the newly established center-of-excellence at Stockholm University